Mamm Genome (2015) 26:222–234
DOI 10.1007/s00335-015-9560-4

Cystic fibrosis mouse model-dependent intestinal structure and gut microbiome

Mark Bazett · Lisa Honeyman · Anguel N. Stefanov · Christopher E. Pope · Lucas R. Hoffman · Christina K. Haston

Received: 21 December 2014 / Accepted: 13 February 2015 / Published online: 27 February 2015

Abstract Mice with a null mutation in the cystic fibrosis transmembrane conductance regulator (*Cftr*) gene show intestinal structure alterations and bacterial overgrowth. To determine whether these changes are model-dependent and whether the intestinal microbiome is altered in cystic fibrosis (CF) mouse models, we characterized the ileal tissue and intestinal microbiome of mice with the clinically common ΔF508 *Cftr* mutation (FVB/N *Cftr*^{tm1Eur}) and with *Cftr* null mutations (BALB/c *Cftr*^{tm1UNC} and C57BL/6 *Cftr*^{tm1UNC}). Intestinal disease in 12-week-old CF mice, relative to wild-type strain controls, was measured histologically. The microbiome was characterized by pyrosequencing of the V4–V6 region of the 16S rRNA gene and intestinal load was measured by RT-PCR of the 16S rRNA gene. The CF-associated increases in ileal crypt to villus axis distention, goblet cell hyperplasia, and muscularis externa thickness were more severe in the BALB/c and C57BL/6 *Cftr*^{tm1UNC} mice than in the FVB/N *Cftr*^{tm1Eur} mice. Intestinal bacterial load was significantly increased in all CF models, compared to levels in controls, and positively correlated with circular muscle thickness in CF, but not wild-type, mice. Microbiome profiling identified *Bifidobacterium* and groups of *Lactobacillus* to be of altered abundance in the CF mice but overall bacterial frequencies were not common to the three CF strains and were not correlative of major histological changes. In conclusion, intestinal structure alterations, bacterial overgrowth, and dysbiosis were each more severe in BALB/c and C57BL/6 *Cftr*^{tm1UNC} mice than in the FVB/N *Cftr*^{tm1Eur} mice. The intestinal microbiome differed among the three CF mouse models.

Introduction

Cystic fibrosis (CF) is an autosomal recessive disease caused by defects in the cystic fibrosis transmembrane conductance regulator (*CFTR*) gene. Although over 1500 different mutations in *CFTR* have been documented, a deletion of a phenylalanine at position 508 (ΔF508) accounts for 70 % of those found among people with CF (O'Sullivan and Freedman 2009). CF patients have well-described pathologies affecting the lung and pancreas, and can also develop intestinal disease which manifests as meconium ileus and distal intestinal obstruction syndrome in this population (van der Doef et al. 2011). Small intestinal bacterial overgrowth has been reported as a feature of clinical CF intestinal disease (Lisowska et al. 2009).

Intestinal phenotypes resembling meconium ileus (Snouwaert et al. 1992) and distal intestinal obstruction syndrome (Durie et al. 2004) develop in mice with a null mutation in *Cftr* (*Cftr*^{tm1Unc} mice) and in the mice these traits are characterized by mucous build up and the presence of lethal intestinal plugs (Durie et al. 2004; Snouwaert

Electronic supplementary material The online version of this article (doi:10.1007/s00335-015-9560-4) contains supplementary material, which is available to authorized users.

M. Bazett · L. Honeyman · A. N. Stefanov · C. K. Haston (✉)
Meakins-Christie Laboratories, Departments of Medicine and Human Genetics, McGill University, 3626 St. Urbain, Montreal, QC H2X 2P2, Canada
e-mail: christina.haston@mcgill.ca

C. E. Pope · L. R. Hoffman
Department of Pediatrics, University of Washington School of Medicine, Seattle, WA, USA

L. R. Hoffman
Department of Microbiology, University of Washington School of Medicine, Seattle, WA, USA

et al. 1992). Histologically, *Cftr*^{tm1Unc} mice, on either the C57BL/6 J (Durie et al. 2004; Kent et al. 1996) or BALB/cJ (Bazett et al. 2011; Canale-Zambrano et al. 2010) genetic background, have intestinal goblet cell hyperplasia, and crypt dilation and elongation. Our studies of C57BL/J x BALBc/J F2 *Cftr*^{tm1Unc} mice also demonstrated the intestinal submucosa to be thicker in the Cftr-deficient mice (Canale-Zambrano and Haston 2011). Finally, intestinal bacterial overgrowth is a feature of the *Cftr*^{tm1Unc} model (Canale-Zambrano et al. 2010; Clarke et al. 2004; Norkina et al. 2004).

In addition to *Cftr*^{tm1Unc} mice, cystic fibrosis has been modeled with FVB/N *Cftr*^{tm1Eur} mice (van Doorninck et al. 1995) which carry the clinically common ΔF508 mutation. These mice express the mutant allele at the same level at which wild-type (WT) mice express the wild-type allele in assayed tissues including the intestine (French et al. 1996). This CF mouse model has been used to assay CFTR function in the lung (Gavina et al. 2013; Lubamba et al. 2009), salivary glands (Droebner and Sandner 2013) and intestine (Dekkers et al. 2013; Dhooghe et al. 2013) but the intestinal disease in these mice has not been quantified. An early report indicated *Cftr*^{tm1Eur} mice to have an intestinal phenotype of goblet cell hyperplasia with limited crypt distention and intestinal obstructions (van Doorninck et al. 1995), at 5–7 weeks of age, but the extent of disease in adults, and whether *Cftr*^{tm1Eur} mice also develop bacterial overgrowth is unknown.

The bacterial overgrowth phenotype is potentially of interest to the development of CF pathology in the intestine but clinical studies of this interaction are likely to be confounded by the prevalence of antibiotic treatment in the CF patient population. Specifically, non-CF studies have shown that the introduction of specific bacteria to mice can result in increased crypt depth (Preidis et al. 2012), and that gastroenterological patients with small intestinal bacterial overgrowth also have a decreased villus to crypt ratio (Lappinga et al. 2010) which is consistent with the CF intestinal change. High throughput microbiome sequencing has been applied to CF, most commonly of respiratory samples, and has shown there to be an effect of antibiotic treatment on the pulmonary microbiome (Zhao et al. 2012). The clinical CF intestinal microbiome has not been characterized, but limited investigation of fecal samples from CF patients (Duytschaever et al. 2011, 2013; Hoffman et al. 2014; Lynch et al. 2013; Scanlan et al. 2012) has suggested an intestinal dysbiosis exists, and features alterations in the abundance of individual bacterial groups including *Bifidobacterium* (Duytschaever et al. 2013; Scanlan et al. 2012) and *Escherichia coli* (Hoffman et al. 2014), which may be associated with disease (Hoffman et al. 2014). An evaluation of the intestinal microbiome of the differing CF mouse models has not been completed.

CF mouse models thus recapitulate important aspects of the gastrointestinal pathology observed in patients and can be studied in the absence of antibiotics. The current study was undertaken to determine whether differences exist in the intestinal disease phenotype among three different CF mouse models- BALB/c *Cftr*^{tm1Unc}, C57BL/6 *Cftr*^{tm1Unc} and FVB/N *Cftr*^{tm1Eur} mice, and, if so, to investigate whether these changes are associated with specific constituents of the intestinal microbiome.

Materials and methods

Mice

Cftr+/^{tm1Eur} heterozygous mice (van Doorninck et al. 1995), which had been backcrossed for 13 generations to the FVB/N strain, were obtained from Dr. B. Scholte of the Erasmus University Medical Centre Rotterdam, the Netherlands. These mice were bred together to produce *Cftr*^{tm1Eur} mice and wild-type *Cftr* +/+ controls and were genotyped as previously described (Paradis et al. 2010), *Cftr*$^{+/tm1UNC}$ heterozygous mice on either C57BL/6 or BALB/c background were used to generate knockout (*Cftr*^{tm1UNC}) mice as previously described (Bazett et al. 2012; Haston et al. 2006). All mice were bred and maintained at the Meakins-Christie Laboratories of McGill University. To circumvent possible premature death due to intestinal disease, all mice (CF and WT) were fed standard chow and received PEGLYTE® (17.8 mmol/L polyethylene glycol, Pharma Science, DIN:00777838) in their drinking water as described previously (Bazett et al. 2012; Clarke et al. 1996; Haston et al. 2006; Paradis et al. 2010). Mice were weaned at 3 weeks of age and grouped in ventilated cages of 1–3 mice based on their sex. CF and WT mice were co-housed. At 12 weeks of age the mice were weighed and euthanized with a lethal dose of anesthetic. At dissection, the entire small intestine was removed, flushed with phosphate buffered saline containing a mucolytic agent (10 mM dithiothreitol), the contents collected, and the tissue was fixed in formalin before being submitted for standard histological processing. All animal procedures were performed in accordance with McGill University guidelines set by the Canadian Council on Animal Care.

Histology

Paraffin-embedded Sects. (5 μm) were stained with hematoxylin and eosin for evaluation of general histological structure. The crypt to villus axis (CVA) height was measured, from 25 complete and intact CVAs within each ileum, using image analysis of the histological sections

(Olympus BX51, Image-Pro Plus 5.1, Media Cybernetics) as in previous studies (Bazett et al. 2011; Canale-Zambrano et al. 2010; Canale-Zambrano et al. 2007). Separate measurements of villus height and crypt depth were also taken. The number of goblet cells was counted for an average of 20–25 CVAs per section from Periodic acid-Schiff/Alcian blue stained sections. For muscle thickness, both the circular and longitudinal muscle layers of the muscularis externa were measured at 50 regular intervals throughout the section, and nuclei per mm^2 were enumerated in ten regions located throughout the section. All sections were scored by an observer blinded to mouse strain and *Cftr* genotype.

Bacterial load measurement

DNA for bacterial load quantification was extracted from 200 mg of the centrifuged small intestinal contents using a Stool DNA Kit (Qiagen, #51504). The bacterial load was quantified by real-time PCR amplification of the 16S (small ribosomal subunit) gene as previously described (Canale-Zambrano et al. 2010; Ott et al. 2004). A standard curve of the number of 16S rRNA gene copies present was created by extracting and quantifying DNA from a known number of *E. coli* D5Hα, which has seven 16S rRNA copies per bacteria.

Bacterial DNA extraction and PCR amplification of the 16S rRNA gene

DNA was isolated from small intestinal contents by repeated bead beating followed by a column extraction as previously described (Hoffman et al. 2014; Yu and Morrison 2004). FLX Pyrosequencing of the V4–V6 variable region of the bacterial 16S rRNA gene (Primers: 530-F: GTGCCAGC MGCNGCGG and 1100-R: GGGTTNCGNTCGTTG) was completed by MrDNA as previously described (Dowd et al. 2008). 10,000 reads were sequenced per sample and a total of 548,576 reads were collected. Raw sequences were analyzed using Mothur (Schloss et al. 2009) version 1.28, a publicly available online computational microbiomics resource which has previously been used to analyze the microbiome in CF patients (Zhao et al. 2012) and mice (Russell et al. 2012), with a pipeline similar to that described previously (Schloss et al. 2011). Raw sequences were cleaned using the Mothur implementation of PyroNoise (Quince et al. 2009) and analyzed sequences were retained based on read lengths of >200 bp, fewer than two barcode mismatches, fewer than three primer mismatches and no homopolymer stretches >8 nucleotides. Sequences were aligned using the SILVA reference database (Pruesse et al. 2007) and unique sequences were defined as having no more than two bases apart. Chimeras were removed using the Mothur implementation of UChime (Edgar et al. 2011). The resulting 355,187 sequences were assigned to operational taxonomic units (OTUs) based on 97 % sequence similarity with the most abundant read serving as the representative read. Taxonomic assignment of reads was completed with the Ribosomal Database Project classifier (Wang et al. 2007). The sequencing data was rarefied to 5457 sequences per sample.

Statistical analysis

Weight, histological and bacterial load phenotypes are expressed as the mean ± SD and differences in phenotype between mice grouped by *Cftr* genotype were determined using Student's *t* test. To assess the significance of differences among models, ANOVA was used with Tukey's post hoc test. Correlations between bacterial load and histological features were defined with Pearson's correlation coefficient.

Phylogenetic trees were constructed using Clearcut (Evans et al. 2006) via Mothur. Alpha diversity, Chao1 richness estimator, Simpson Evenness and Shannon's Diversity were calculated in Mothur (Schloss et al. 2009). Correlations between these population measures and phenotypes of histological features, bacterial load and body weight were defined with Pearson's correlation coefficient. To investigate the compositional similarity between samples, Bray-Curtis dissimilarities were calculated for each model, data were visualized using two dimensional nonmetric dimensional scaling (NMDS) ordination, and significant differences between groups were determined by Adonis, using vegan package 2.0–10 in R (http://CRAN.R-project.org/package=vegan). Differences in abundance of OTUs between mice grouped by *Cftr* genotype were determined by the Mothur implementation of the Metastats program (White et al. 2009). The abundance of OTUs which had reads in more than two CF mice was correlated with histological features and with body weight. Correlations were completed on the CF mice with all three strains considered together and were evaluated using Pearson's correlation coefficient with the Bonferroni-corrected $P < 0.0011$ taken as the level of significance.

Results

Survival and body weight phenotype

A population of mice was bred from a cross of FVB/N *Cftr*+/^{tm1Eur} progenitors and of the mice produced 28 % were homozygous for the ΔF508-*Cftr* allele at weaning, which is consistent with expected Mendelian ratios. Greater than 89 % of *Cftr*^{tm1Eur} mice survived to the experimental age of 12 weeks and no intestinal blockages

were apparent at necropsy. As seen in Fig. 1a, the average weight of the *Cftr*^{tm1Eur} mice at 12 weeks of age was not significantly different from that of wild-type controls ($P = 0.11$), in agreement with previous data of this strain (Bazett and Haston 2014; Paradis et al. 2010). This is in contrast to *Cftr*^{tm1UNC} mice, also bred from heterozygous progenitors, which had less than the expected 25 % homozygous *Cftr*^{tm1UNC} mouse production rates at weaning (BALB/c = 9.2 %, C57BL/6 = 6.9 %). *Cftr*^{tm1UNC} mice were significantly smaller than controls for BALB/c ($P = 0.0008$), and C57BL/6 ($P = 0.04$) strains, in agreement with previous reports (Bazett et al. 2011; Canale-Zambrano et al. 2010; Haston et al. 2002; Norkina et al. 2004). There was a significant difference in weight among the strains of CF mice with the FVB/N *Cftr*^{tm1Eur} mice weighing more than the BALB/c *Cftr*^{tm1UNC} mice. The strain-dependent difference in body weight among CF mice was not evident within the wild-type mice; Fig. 1a.

Ileal histology

To determine whether adult FVB/N mice with the ΔF508 mutation in *Cftr* presented with intestinal disease, and if so, how this intestinal disease related to that of *Cftr*^{tm1UNC} mice, measures of crypt-villus axis (CVA) height, muscularis externa thickness, and goblet cell count were made in ileal tissue procured from FVB/N *Cftr*^{tm1Eur}, BALB/c *Cftr*^{tm1UNC}, C57BL/6 *Cftr*^{tm1UNC}, and wild-type control mice. As shown in Fig. 1b–d, the ilea of each of the three CF mouse models contained significantly more goblet cells per CVA than those of wild-type control mice ($P = 0.001$ for FVB/N; $P = 8.4 \times 10^{-6}$ for BALB/c, $P = 6.4 \times 10^{-5}$ for C57BL/6). Among the CF models, there was a significant difference in goblet cell hyperplasia, with FVB/N *Cftr*^{tm1Eur} mice having fewer goblet cells per CVA than the BALB/c *Cftr*^{tm1UNC} mice. This trait did not vary by strain in wild-type mice, as shown in Fig. 1b.

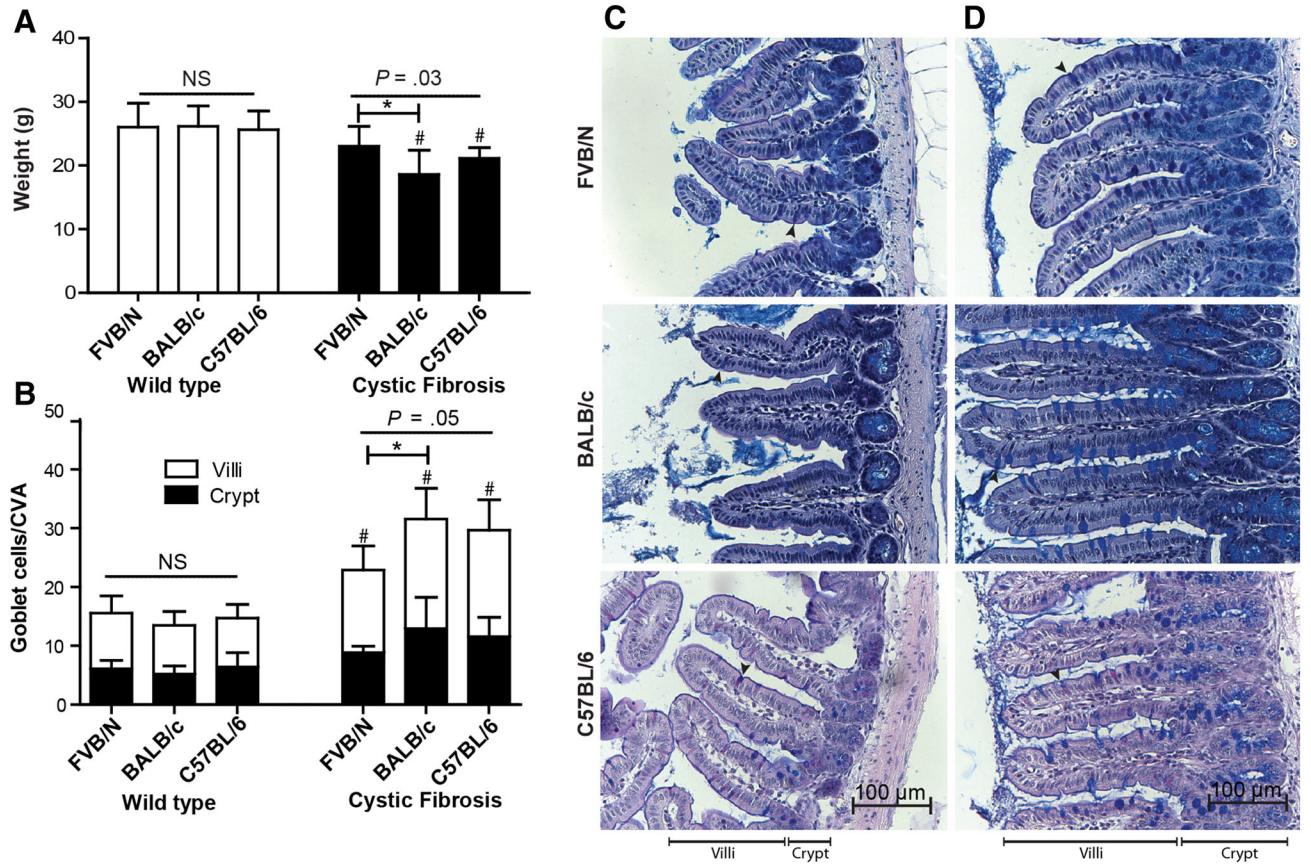

Fig. 1 Body weight and ileal goblet cell counts of FVB/N *Cftr*^{tm1Eur}, BALB/c *Cftr*^{tm1UNC}, C57BL/6 *Cftr*^{tm1UNC}, and WT control mice at 12 weeks of age. **a** Weights of mice at sacrifice. **b** Number of goblet cells per crypt to villus axis (CVA), (villus *open square*; crypt *filled square*). Data are presented as the mean ± SD ($n = 5$–13 mice/group). *Horizontal bars* indicate groups compared by ANOVA (*NS* not significant). *Indicates a significant difference, $P < 0.05$, by Tukey's post hoc test. # Indicates a significant difference, $P < 0.05$, between CF and WT mice within each strain by Student's *t* test. Representative ileal sections of **c** a wild-type control mouse from each strain, and **d** FVB/N *Cftr*^{tm1Eur}, BALB/c *Cftr*^{tm1UNC} and C57BL/6 *Cftr*^{tm1UNC} mice featuring hyperplasia of goblet cells (*arrows*). Periodic acid-Schiff//Alcian Blue stain, magnification ×400

Secondly, the average CVA height in all three CF mouse models exceeded that of wild-type mice ($P = 0.004$ for FVB/N; $P = 3.6 \times 10^{-6}$ for BALB/c, $P = 6.4 \times 10^{-6}$ for C57BL/6; Fig. 2a, b). The CVA height did not differ by strain among wild-type mice, but in the CF mice the CVA distention of FVB/N *Cftr*^{tm1Eur} mice was significantly reduced compared to that of the BALB/c *Cftr*^{tm1UNC} and C57BL/6 *Cftr*^{tm1UNC} mice; Fig. 2c.

Finally, to investigate whether the ΔF508 mutation in *Cftr* caused an increase in the muscularis externa layer of the ileum, and how this compared to the null mutation models of *Cftr,* measurements of the muscle layers in the

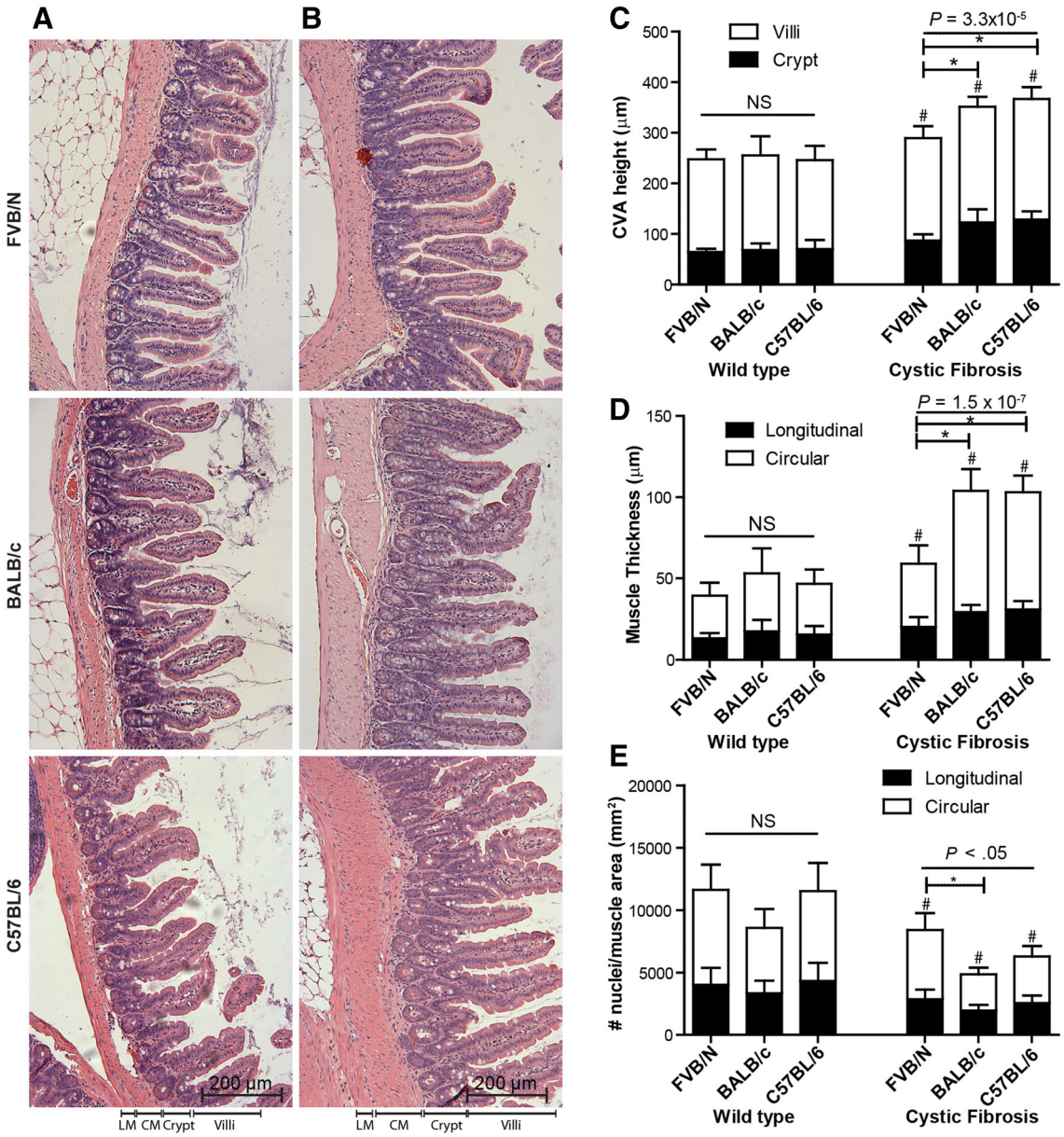

Fig. 2 Crypt to villus axis (CVA) height and muscularis externa thickness and cell density of the ileal tissue of FVB/N *Cftr*^{tm1Eur}, BALB/c *Cftr*^{tm1UNC}, C57BL/6 *Cftr*^{tm1UNC}, and WT control mice at 12 weeks of age. Representative ileal sections of **a** a wild-type control mouse from each strain, and **b** FVB/N *Cftr*^{tm1Eur}, BALB/c *Cftr*^{tm1UNC} and C57BL/6 *Cftr*^{tm1UNC} mice showing distended CVA and increased muscle thickness. Hematoxylin and Eosin stain, magnification ×200. *LM* longitudinal muscle, *CM* circular muscle. **c** CVA height, (villus *open square*; crypt *filled square*) was measured by image analysis of histological sections for 25 ileal CVAs per mouse. **d** Muscle layer thickness was measured by image analysis of ileal histological sections (longitudinal muscle *filled square*; circular muscle *open square*) *LM* longitudinal muscle, *CM* circular muscle. **e** Number of nuclei per unit area (mm^2) of muscularis externa. Data are presented as the mean ± SD (n = 5–13 mice/group); *Horizontal bars* indicate groups compared by ANOVA (*NS* not significant). *Indicates a significant difference, $P < 0.05$, by Tukey's post hoc test. # Indicates a significant difference, $P < 0.05$, between CF and WT mice within each strain by Student's t test

ileal tissue were completed in these mice. As shown in Fig. 2, both the circular and longitudinal muscle layers of the muscularis externa in the ileum were significantly thicker in the FVB/N *Cftr*^{tm1Eur}, BALB/c *Cftr*^{tm1UNC} and C57BL/6 *Cftr*^{tm1UNC} mice compared to strain controls ($P = 0.005$ for FVB/N; $P = 2.2 \times 10^{-7}$ for BALB/c, $P = 2.8 \times 10^{-7}$ for C57BL/6). Among strains, there was no difference in total muscle thickness for the wild-type mice, but there was a significant difference in this trait for CF mouse models ($P = 1.5 \times 10^{-7}$) wherein the total muscle layer thickness, circular muscle thickness, and longitudinal muscle thickness were each significantly reduced in the FVB/N ΔF508 mice compared to the *Cftr*^{tm1UNC} models; Fig. 2d. Finally, tissue from all three CF mouse models had significantly fewer nuclei per mm^2 of muscularis externa compared to controls, indicating that hypertrophy of smooth muscle cells contributed to the increased muscle thickness; Fig. 2e.

Bacterial load quantification

To determine whether the CF mouse models presented with similar increases in bacterial load, the intestinal contents from FVB/N *Cftr*^{tm1Eur}, BALB/c *Cftr*^{tm1UNC}, C57BL/6 *Cftr*^{tm1UNC}, and wild-type control mice were evaluated with quantitative real time RT-PCR. As shown in Fig. 3a, all three CF mouse models had significantly increased bacterial density compared to the levels in wild-type strain controls ($P = 0.044$ for FVB/N; $P = 0.006$ for BALB/c, $P = 0.018$ for C57BL/6). While the bacterial load was similar in all strains of wild-type mice, there was a significant difference by strain in the CF mice, with bacterial loads in C57BL/6 *Cftr*^{tm1UNC} mice significantly exceeding those of FVB/N *Cftr*^{tm1Eur} mice. The bacterial load of BALB/c *Cftr*^{tm1UNC} mice was not significantly different from that of either of FVB/N *Cftr*^{tm1Eur} mice or C57BL/6 *Cftr*^{tm1UNC} mice.

To determine whether bacterial load was related to extent of histological disease, correlation analyses were performed. Bacterial load was significantly correlated with circular muscle thickness ($r = 0.36$; $P = 0.04$), in CF, but not WT, mice as illustrated in Fig. 3b, c. There was also a suggestive, but non-significant, correlation between bacterial load and CVA height in CF mice ($r = 0.31$; $P = 0.09$, data not shown). Neither goblet cell count per CVA nor body weight of CF mice correlated significantly with bacterial load ($P > 0.22$, data not shown).

Intestinal microbiome of CF mice

To investigate whether the bacterial microbiome within the small intestine differed among mice grouped by *Cftr* genotype within each strain, DNA extracted from intestinal

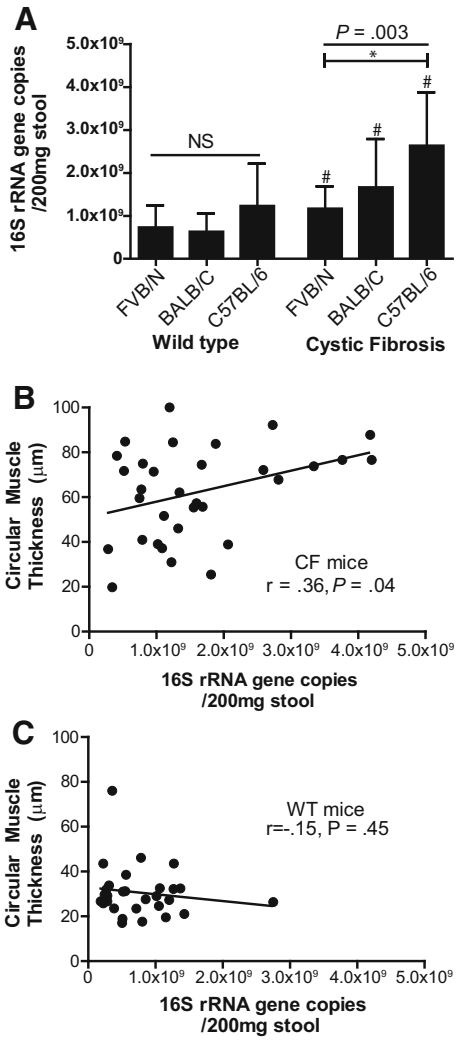

Fig. 3 Small intestinal bacterial load of FVB/N *Cftr*^{tm1Eur}, BALB/c *Cftr*^{tm1UNC}, C57BL/6 *Cftr*^{tm1UNC}, and WT control mice at 12 weeks of age and correlation to circular muscle thickness. **a** Bacterial load was measured using quantitative RT-PCR of the 16S rRNA of DNA isolated from small intestinal contents. Average ± SD is shown ($n = 7$–14 mice/group). *Horizontal bars* indicate groups compared by ANOVA (*NS* not significant). *Indicates a significant difference, $P < 0.05$, by Tukey's post hoc test. # Indicates a significant difference, $P < 0.05$, between CF and WT mice within each strain by Student's *t* test. Correlation between bacterial load and circular muscle thickness in **b** CF mice ($n = 8$–13 per strain) and **c** WT mice ($n = 7$–13 per strain)

content samples was evaluated by 454 pyrosequencing of the V4–V6 region of the bacterial 16S rRNA gene.

The effect of a *Cftr* mutation on the overall compositional similarity for each strain was investigated using Bray-Curtis dissimilarity and is presented in Fig. 4a–c with two dimensional non-metric multidimensional scaling (NMDS). As seen in this figure, samples from FVB/N *Cftr*^{tm1Eur} mice clustered with those from FVB/N wild-type mice (Adonis test, $P = 0.20$) as did samples from BALB/c

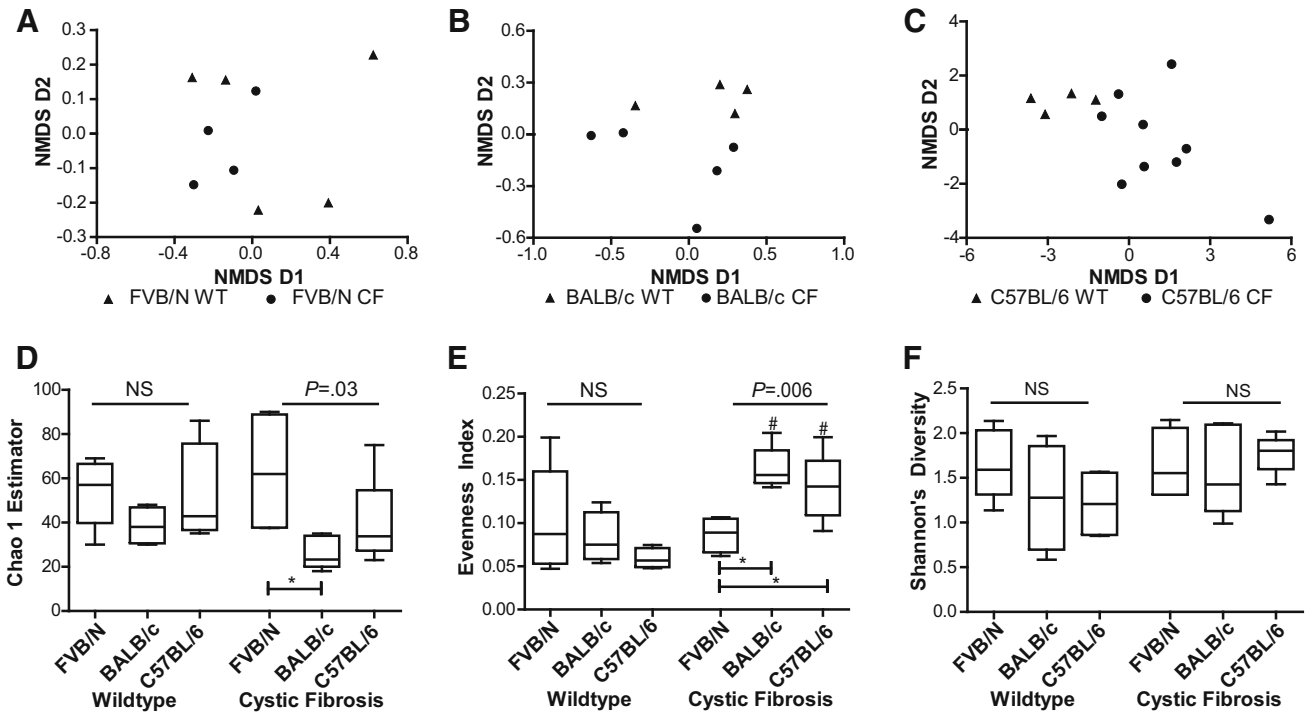

Fig. 4 Small intestinal microbiome community metrics for FVB/N *Cftr*^{tm1Eur}, BALB/c *Cftr*^{tm1UNC}, C57BL/6 *Cftr*^{tm1UNC}, and WT control mice. Two dimensional non-metric multidimensional scaling (NMDS) of the Bray-Curtis dissimilarity between samples for **a** FVB/N *Cftr*^{tm1Eur} mice, **b** BALB/c *Cftr*^{tm1UNC} mice, **c** C57BL/6 *Cftr*^{tm1UNC} mice, and respective wild-type mice. **d** Richness was measured using the Chao 1 estimator. **e** Evenness defined by Simpson's Evenness. **f** Diversity, measured with Shannon's Diversity Index. Data are presented as mean ± SD ($n = 4$–9 per group). *Horizontal bars* indicate groups compared by ANOVA (*NS* not significant). *Indicates a significant difference, $P < 0.05$, by Tukey's post hoc test. # Indicates a significant difference, $P < 0.05$, between CF and WT mice within each strain by Student's *t* test

Cftr^{tm1UNC} with their in strain wild-type mice (Adonis test, $P = 0.14$). C57BL/6 *Cftr*^{tm1UNC} derived samples clustered separately from C57BL/6 wild-type-derived samples (Adonis test $P = 0.002$).

Next, we determined whether there were community structure differences in the intestinal microbiome either between each line of CF mice and respective controls, or among the CF models. Richness, which represents the number of microbial taxa in a sample, was calculated with the Chao 1 estimator. This parameter was decreased ($P = 0.06$) in samples from BALB/c *Cftr*^{tm1UNC} mice, but not in FVB/N *Cftr*^{tm1Eur} ($P = 0.60$) or C57BL/6 *Cftr*^{tm1UNC} ($P = 0.41$) mice, when compared to in strain controls, as shown in Fig. 4d. Further, there was a significant difference in the Chao 1 estimates among the CF models, which was not evident within the wild-type mice, as the FVB/N *Cftr*^{tm1Eur} mice were estimated to have greater richness than the BALB/c *Cftr*^{tm1UNC} mice. Community evenness, or the relative distribution of taxa within the samples, was evaluated with Simpsons Evenness Index. As shown in Fig. 4e, community evenness was significantly increased compared to controls in samples from BALB/c *Cftr*^{tm1UNC} ($P = 0.005$) and C57BL/6 *Cftr*^{tm1UNC} mice ($P = 0.0001$) but not from FVB/N *Cftr*^{tm1Eur} mice ($P = 0.61$). Variability in evenness among CF mouse strains, but not wild-type mice, was also evident, as the FVB/N *Cftr*^{tm1Eur} mice differed from the BALB/c and C57BL/6 *Cftr*^{tm1UNC} mice for this parameter. Diversity, a combination of the richness and evenness of a population, which was measured with Shannon's index, was higher ($P = 0.06$), in samples from C57BL/6 *Cftr*^{tm1UNC} mice relative to wild-type levels. No differences in diversity were evident for comparisons between any of the remaining wild-type or CF mouse strains, as illustrated in Fig. 4f.

To determine whether any of the microbiome community measures was related to extent of histological disease, body weight, or to bacterial load, correlation analyses were performed. The histological features of CVA height ($r = 0.60$; $P = 0.008$), goblet cells/CVA ($r = 0.57$; $P = 0.014$), circular muscle thickness ($r = 0.65$; $P = 0.003$), longitudinal muscle thickness ($r = 0.55$; $P = 0.018$), circular muscle cell density ($r = -0.70$; $P = 0.001$), and longitudinal muscle cell density ($r = -0.54$; $P = 0.018$) were each correlated with Simpson's evenness index in CF, but not WT, mice as shown in Supplemental Fig. 1. Similarly, the richness measure (Chao1) was suggestively to significantly correlated with intestinal disease in CF mice, as illustrated in

Supplemental Fig. 2, while not correlated in WT mice, with the possible exception of Chao 1 estimates correlated to goblet cells/CVA (r = 0.51; $P = 0.09$) in intestines of WT mice. Shannon's Diversity measures were not significantly correlated with the histological features in CF or WT mice ($P > 0.19$), data not shown, but were correlated ($r = 0.51$; $P = 0.09$) to bacterial load in CF ($r = 0.67$; $P > 0.009$), but not WT mice ($P = 0.24$), data not shown. None of the microbiome community measures was related to body weight in either of CF ($P > 0.33$), or WT mice ($P > 0.17$), data not shown.

Regarding the microbiome composition, for both the CF and wild-type mice of each of the three strains, the major phyla present were Firmicutes, Actinobacteria and Proteobacteria (Fig. 5), in agreement with the expected microbiome in mouse intestines (Hildebrand et al. 2013; Ivanov et al. 2009; O'Connor et al. 2014; Rehman et al. 2011; Russell et al. 2012). At the phylum level C57BL/6 *Cftr*^{tm1UNC} mice had a significantly decreased abundance of Firmicutes ($P = 0.02$) and an increased abundance of Actinobacteria ($P = 0.003$), compared to levels in C57BL/6 WT mice. While similar trends in those two phyla were apparent in the other models, BALB/c *Cftr*^{tm1UNC} and FVB/N *Cftr*^{tm1Eur} mice did not have significantly altered abundances of specific bacteria at the phylum level when compared to wild-type mice.

Further, to investigate whether specific taxa within the phyla were affected by the Cftr deficiency, the 16S rRNA gene reads were mapped into operational taxonomic units (OTUs). As shown in Fig. 5b and Table 1, OTUs which were largely specific to each model differed in abundance between samples from CF and wild-type mice of each strain. The relative abundance of an OTU corresponding to *Bifidobacterium* was the only bacterial group increased in CF mice of all three strains (FVB/N, $P = 0.04$; BALB/c, $P = 0.07$; C57BL/6, $P = 0.002$) compared to wild-type levels. In FVB/N *Cftr*^{tm1Eur} mice, the other major microbiome difference was increased levels of an OTU corresponding to a group of *Lactobacillus*, compared to levels in FVB/N wild-type mice. In the BALB/c strain, two distinct OTUs that both corresponded to *Lactobacillus* were altered in abundance between *Cftr*^{tm1UNC} and wild-type mice. In C57BL/6 mice, OTUs for *Lactobacillus* and *Erysipelotrichaceae*, were of altered abundance in mice grouped by *Cftr*^{tm1UNC} genotype.

We analyzed whether the intestinal abundance of specific bacteria was correlative of the CF traits. In this analysis, the correlation for each OTU detected in more than two CF mice was completed, using data from the CF mice of all three strains considered together. This investigation of OTU abundance with each of the histological features, and with the phenotype of body weight, revealed no significant correlations after correction for multiple testing between OTU frequencies and traits of CVA distension, goblet cell hyperplasia, and muscle thickness in CF mice ($P > 0.002$, data not shown). A significant correlation between the number of nuclei per mm^2 in the circular muscle layer and OTU17, which corresponds to an unclassified Porphyromonadaceae ($r = 0.82$; $P < 0.0001$) was detected.

Discussion

Our investigation of intestinal disease in CF mice revealed all three models to develop bacterial overgrowth with histological features of crypt to villus axis distention, goblet cell hyperplasia, and increased muscle thickness. Secondly these traits, although significantly increased compared to measures from wild type, were less severe in adult FVB/N *Cftr*^{tm1Eur} mice relative to BALB or C57BL/6 J *Cftr*^{tm1UNC} mice. Finally, microbiome profiling identified CF intestinal dysbiosis to be model specific in mice.

CF related intestinal structure changes were evident in all models, and these phenotypes were reduced in magnitude in the FVB/N ΔF508 mice. Indeed, the extent of CVA distention and goblet cell hyperplasia reported here agree well with prior findings for BALB/c (Bazett et al. 2011; Canale-Zambrano et al. 2010) and C57BL/6 (Durie et al. 2004; Kent et al. 1996) *Cftr*^{tm1UNC} mice and the trait of increased intestinal muscle thickness, originally reported in BALB x C57BL/6 J F2 *Cftr*^{tm1UNC} mice (Canale-Zambrano and Haston 2011), was also evident in the BALB/c and C57BL/6 *Cftr*^{tm1UNC} models. The findings of increased longitudinal and circular muscle thickness in the intestines of C57BL/6 *Cftr*^{tm1UNC} mice may contradict those of prior reports (De Lisle et al. 2010; Risse et al. 2012) but as in the latter work normalized area of alpha smooth muscle staining was reported, differences in methods of histological assessment may have contributed to the discrepancy. The intestinal disease measured here had not been comprehensively studied in adult FVB/N ΔF508 mice although indications of goblet cell hyperplasia have been reported (van Doorninck et al. 1995; Wilke et al. 2011) without "dramatic" CVA distention (van Doorninck et al. 1995). The cause of CVA distention in CF mice is unknown but it has been proposed to depend on increased proliferation in the intestinal crypts (Canale-Zambrano and Haston 2011; Gallagher and Gottlieb 2001) which, in turn, may be related to their alkaline environment (Liu et al. 2012; Putney and Barber 2003). The milder CF phenotype of FVB/N ΔF508 mice extended to the microbiome, in terms of population characteristics, where standard metrics for these mice did not differ from those of wild-type mice in contrast to samples from the *Cftr*^{tm1UNC} models. Given how the models were constructed, however, we cannot discern whether the reduced phenotype of FVB/N

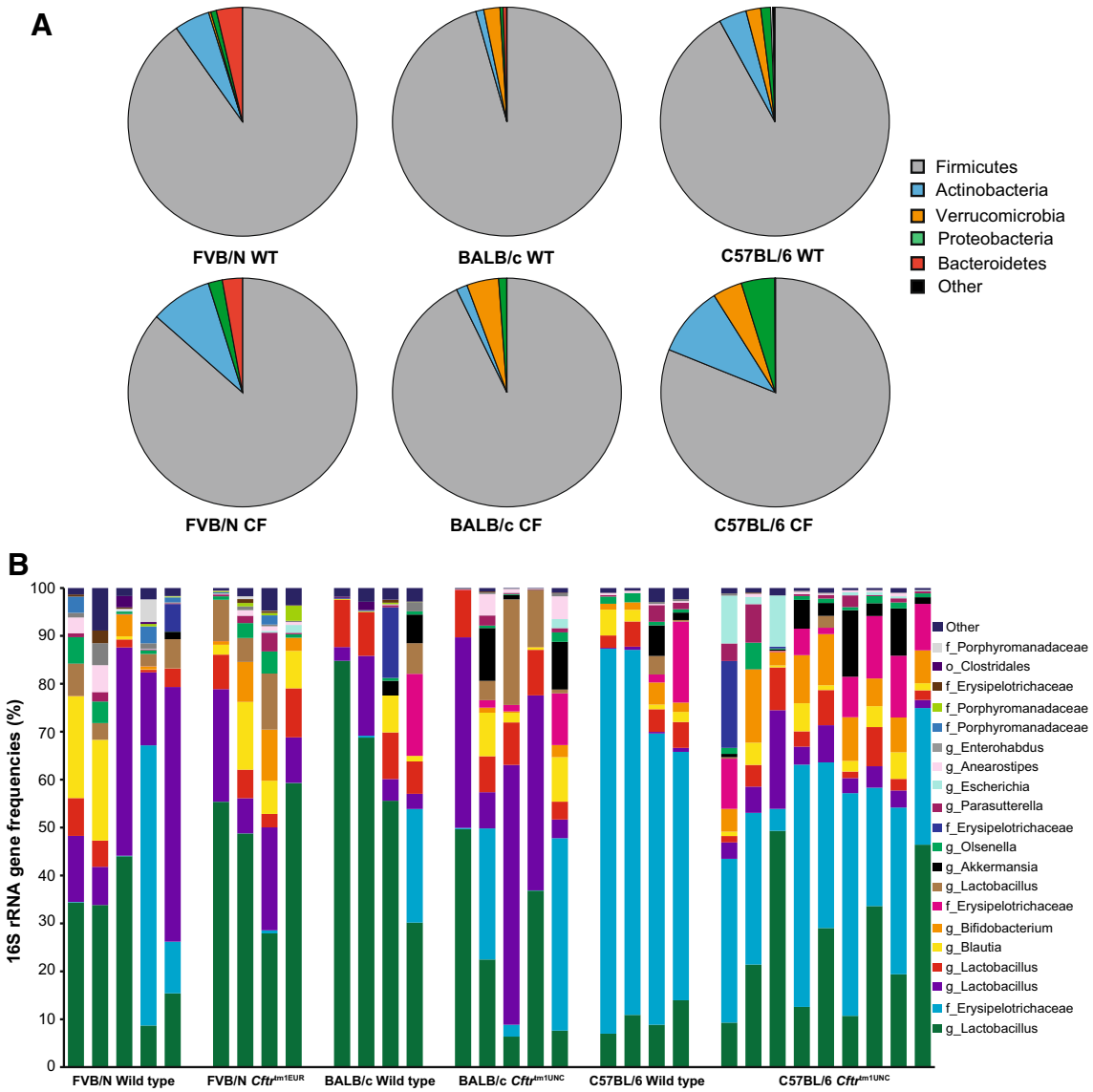

Fig. 5 Small intestinal microbiome community composition of FVB/N *Cftr*^{tm1Eur}, BALB/c *Cftr*^{tm1UNC}, C57BL/6 *Cftr*^{tm1UNC}, and wild-type strain control mice at 12 weeks of age. **a** Phylum level classification. *Firmicutes* were significantly decreased ($P = 0.02$) and *Actinobacteria* ($P = 0.003$) were significantly increased in C57BL/6 *Cftr*^{tm1UNC} mice compared to C57BL/6 WT mice. No other significant differences in bacterial abundance at the genus level, between CF mice and WT in strain controls, were detected. The group "other" contains the phylum Tm7, Tenericutes, Fusobacteria and unclassified bacteria. **b** 16S rRNA gene frequencies of the most abundant operational taxonomic unit (OTU) classified to the closest related taxon. Classifications: *o* order, *f* family, *g* genus

ΔF508 mice, compared to the BALB and C57BL/6 J *Cftr*^{tm1UNC} mice, is the influence of the *Cftr* mutation (ΔF508 compared to *Cftr* null) or of genetic background (FVB/N, BALB, C57BL/6 J) which itself is known to affect both CF traits (Haston et al. 2002), and microbiome composition (Campbell et al. 2012; Hildebrand et al. 2013; O'Connor et al. 2014).

We identified intestinal bacterial overgrowth to be a feature of the *Cftr*^{tm1Eur} model, as it is in *Cftr*^{tm1UNC} mice, and for the circular muscle layer of the intestine to be increased with greater bacterial load in CF mice. The correlation of muscle layer thickness on bacteria may indicate this intestinal phenotype to occur as an adaptive response in CF mice (Barbara et al. 2005). Supporting the potential of an adaptive response wherein muscle layer thickness increases with intestinal bacterial load, parasitic infection of the small intestine of rats has been shown to induce hyperplasia and hypertrophy of intestinal circular muscle (Blennerhassett et al. 1992). Alternatively, as experimentally induced intestinal obstruction is associated with an increased circular muscle layer (Zhao et al. 2010), the correlation of load and muscle thickness in CF mice

Table 1 Operational taxonomic units (OTUs) differing in intestinal abundance between CF and WT mice by nearest classification

Group	Nearest classification	FVB/N WT (%)	FVB/N CF (%)	*P* value	BALB/c WT (%)	BALB/c CF (%)	*P* value	C57BL/6 WT (%)	C57BL/6 CF (%)	*P* value
OTU1	Lactobacillus	27.3 ± 6.5	47.8 ± 7.0	**0.02**	89.9 ± 11.5	24.6 ± 8.4	**0.01**	10.1 ± 1.5	25.8 ± 5.0	**0.008**
OTU2	Erysipelotrichaceae	13.9 ± 11.3	0.18 ± 0.15	0.20	6.0 ± 5.8	14.1 ± 8.3	0.64	67.3 ± 6.6	32.2 ± 4.4	**0.0009**
OTU3	Lactobacillus	26.7 ± 9.0	15.4 ± 4.1	0.23	6.8 ± 3.3	29.2 ± 9.9	**0.03**	0.51 ± 1.5	6.00 ± 1.91	**0.009**
OTU6	Bifidobacterium	1.0 ± 0.9	5.6 ± 2.3	**0.04**	0	0.8 ± 0.4	0.07	2.3 ± 0.8	8.0 ± 1.2	**0.002**
OTU14	Anaerostipes	1.8 ± 1.1	0.7 ± 0.2	0.57	0.03 ± 0.03	2.0 ± 1.1	**0.04**	0.38 ± 0.05	0.31 ± 0.09	0.64
OTU21	Streptococcus	0.23 ± 0.16	0.21 ± 0.16	0.95	0.53 ± 0.23	0.05 ± 0.02	**0.03**	0.055 ± 0.037	0.096 ± 0.040	0.58
OTU29	Clostridium_X1	0.007 ± 0.004	0.160 ± 0.062	**0.01**	0.03 ± 0.03	0.03 ± 0.02	0.90	0.018 ± 0.013	0.047 ± 0.019	0.24
OTU31	Gemella	0	0	N/A	0.43 ± 0.15	0.03 ± 0.01	**0.01**	0.018 ± 0.013	0.0041 ± 0.0041	0.37
OTU35	Erysipelotrichaceae	0.037 ± 0.037	0	0.35	0.009 ± 0.009	0.03 ± 0.03	0.64	0.142 ± 0.045	0.043 ± 0.008	**0.04**
OTU38	Coriobacteriaceae	0.033 ± 0.020	0.032 ± 0.036	0.98	0.03 ± 0.03	0.03 ± 0.02	0.93	0.087 ± 0.029	0.008 ± 0.008	**0.02**

Abundance in % ±SD

Bold values indicate $P < 0.05$

may indicate these traits to be related to developing intestinal obstruction.

The observations of altered smooth muscle thickness, goblet cells, and small bowel bacterial content in the intestines of these mouse models support observations made in people with CF. For example, people with CF tend to have small bowel bacterial overgrowth (Fridge et al. 2007) as well as an abundance of viscid mucous material in the intestinal lumen (Kreda et al. 2012). De Lisle et al. (2010) hypothesized that enteric microbiota impact smooth muscle activity and intestinal transit time through a prostaglandin-dependent mechanism, a pathway which could have contributed to the correlation we observed between muscle thickness and small intestinal bacterial load. Together, these results support close relationships between intestinal mucus secretion, dysbiosis, and dysmotility, indicating that treatments that address one of these abnormalities (e.g., laxatives, antibiotics, and pro kinetic agents, respectively) could positively impact the others and possibly improve overall intestinal function.

In each of the three CF models studied here, the relative abundance of specific CF microbiome constituents was uniquely changed compared to those of wild-type mice. Such variability has also been recorded in CF children (Madan et al. 2012) and CF ferrets (Sun et al. 2014a, b), where intestinal samples from each of studied subjects had a largely unique microbiome profile. This finding may suggest that a dysfunctional or deficient Cftr creates an intestinal environment which includes lower luminal pH (De Lisle et al. 2001), increased transit time (De Lisle 2007), increased mucus production (Malmberg et al. 2006) and abnormal paneth cell dissolution (Clarke et al. 2004) that is permissive for dysbiosis, but does not create a CF specific dysbiosis. The existence of strain-dependent profiles is also likely the reason we were unable to identify specific microbiome constituents which correlated with histological features of intestinal disease in this panel of mice. The intervention used to reduce the incidence of lethal intestinal plugs in the mice, the laxative PEGLYTE, may also have affected the microbiome data observed in CF and WT mice (van der Wulp et al. 2013). Finally, although work to document the CF intestinal and pulmonary microbiomes is ongoing (O'Sullivan and Freedman 2009; Sun et al. 2014a; Zhao et al. 2012, Madan et al. 2012), to date increased *E. coli* levels in fecal samples from CF children (Hoffman et al. 2014) and for the lung, CF-associated bacteria including *Pseudomonas aeruginosa* and *Staphylococcus aureus* (Goddard et al. 2012), as well as *Streptococcus* and *Prevotella* (Filkins et al. 2012) have been reported, these bacteria were not prominent in the samples from CF mice studied here. The lack of commonality is likely due to known microbiome variation by tissue sample site (Costello et al. 2009; Human

Microbiome Project C 2012). The increase in *Bifidobacterium* evident in CF mice may have clinical relevance as it has also been reported as a significant component of the fecal microbiome in CF children (Madan et al. 2012).

In conclusion, mice deficient in Cftr exhibited intestinal structure abnormalities and bacterial overgrowth which were of reduced magnitude in FVB/N *Cftr*^{tm1Eur} mice. Further, in CF mice bacterial overgrowth correlated with the increased circular muscle thickness in the intestine. Our data also support the hypothesis that intestinal microbial dysbiosis is prevalent in CF, and we specifically showed the intestinal microbiome in CF mice to be model-dependent.

Acknowledgments This work was supported by Cystic Fibrosis Canada and the National Institutes of Health (P30 DK089507 and K02 HL105543). Maintenance of the *Cftr*^{tm1Eur} mouse colony at Erasmus MC was supported by the EUROCAFECF EU concerted action program and the Dutch CF Foundation (NCFS).

Disclosures No conflicts to disclose.

References

Barbara G, Stanghellini V, Brandi G, Cremon C, Di Nardo G, De Giorgio R, Corinaldesi R (2005) Interactions between commensal bacteria and gut sensorimotor function in health and disease. Am J Gastroenterol 100:2560–2568

Bazett M, Haston CK (2014) Airway hyperresponsiveness in FVB/N delta F508 cystic fibrosis transmembrane conductance regulator mice. J Cyst Fibros 13:378–383

Bazett M, Paun A, Haston CK (2011) MicroRNA profiling of cystic fibrosis intestinal disease in mice. Mol Genet Metab 103:38–43

Bazett M, Stefanov AN, Paun A, Paradis J, Haston CK (2012) Strain-dependent airway hyperresponsiveness and a chromosome 7 locus of elevated lymphocyte numbers in cystic fibrosis transmembrane conductance regulator-deficient mice. J Immunol 188:2297–2304

Blennerhassett MG, Vignjevic P, Vermillion DL, Collins SM (1992) Inflammation causes hyperplasia and hypertrophy in smooth muscle of rat small intestine. Am J Physiol 262:G1041–G1046

Campbell JH, Foster CM, Vishnivetskaya T, Campbell AG, Yang ZK, Wymore A, Palumbo AV, Chesler EJ, Podar M (2012) Host genetic and environmental effects on mouse intestinal microbiota. ISME J 6:2033–2044

Canale-Zambrano JC, Haston CK (2011) IGF binding protein-3 treatment alters intestinal cell proliferation but not body weight of adult cystic fibrosis transmembrane conductance regulator deficient mice. Pediatr Res 69:129–134

Canale-Zambrano JC, Poffenberger MC, Cory SM, Humes DG, Haston CK (2007) Intestinal phenotype of variable-weight cystic fibrosis knockout mice. Am J Physiol Gastrointest Liver Physiol 293:G222–G229

Canale-Zambrano JC, Auger ML, Haston CK (2010) Toll-like receptor-4 genotype influences the survival of cystic fibrosis mice. Am J Physiol Gastrointest Liver Physiol 299:G381–G390

Clarke LL, Gawenis LR, Franklin CL, Harline MC (1996) Increased survival of CFTR knockout mice with an oral osmotic laxative. Lab Anim Sci 46:612–618

Clarke LL, Gawenis LR, Bradford EM, Judd LM, Boyle KT, Simpson JE, Shull GE, Tanabe H, Ouellette AJ, Franklin CL, Walker NM (2004) Abnormal Paneth cell granule dissolution and compromised resistance to bacterial colonization in the intestine of CF mice. Am J Physiol Gastrointest Liver Physiol 286:G1050–G1058

Costello EK, Lauber CL, Hamady M, Fierer N, Gordon JI, Knight R (2009) Bacterial community variation in human body habitats across space and time. Science 326:1694–1697

De Lisle RC (2007) Altered transit and bacterial overgrowth in the cystic fibrosis mouse small intestine. Am J Physiol Gastrointest Liver Physiol 293:G104–G111

De Lisle RC, Isom KS, Ziemer D, Cotton CU (2001) Changes in the exocrine pancreas secondary to altered small intestinal function in the CF mouse. Am J Physiol Gastrointest Liver Physiol 281:G899–G906

De Lisle RC, Sewell R, Meldi L (2010) Enteric circular muscle dysfunction in the cystic fibrosis mouse small intestine. Neurogastroenterol Motil 22:341–e87

Dekkers JF, Wiegerinck CL, de Jonge HR, Bronsveld I, Janssens HM, de Winter-de Groot KM, Brandsma AM, de Jong NW, Bijvelds MJ, Scholte BJ, Nieuwenhuis EE, van den Brink S, Clevers H, van der Ent CK, Middendorp S, Beekman JM (2013) A functional CFTR assay using primary cystic fibrosis intestinal organoids. Nat Med 19:939–945

Dhooghe B, Noel S, Bouzin C, Behets-Wydemans G, Leal T (2013) Correction of chloride transport and mislocalization of CFTR protein by vardenafil in the gastrointestinal tract of cystic fibrosis mice. PLoS ONE 8:e77314

Dowd SE, Wolcott RD, Sun Y, McKeehan T, Smith E, Rhoads D (2008) Polymicrobial nature of chronic diabetic foot ulcer biofilm infections determined using bacterial tag encoded FLX amplicon pyrosequencing (bTEFAP). PLoS ONE 3:e3326

Droebner K, Sandner P (2013) Modification of the salivary secretion assay in F508del mice—the murine equivalent of the human sweat test. J Cyst Fibros 12:630–637

Durie PR, Kent G, Phillips MJ, Ackerley CA (2004) Characteristic multiorgan pathology of cystic fibrosis in a long-living cystic fibrosis transmembrane regulator knockout murine model. Am J Pathol 164:1481–1493

Duytschaever G, Huys G, Bekaert M, Boulanger L, De Boeck K, Vandamme P (2011) Cross-sectional and longitudinal comparisons of the predominant fecal microbiota compositions of a group of pediatric patients with cystic fibrosis and their healthy siblings. Appl Environ Microbiol 77:8015–8024

Duytschaever G, Huys G, Bekaert M, Boulanger L, De Boeck K, Vandamme P (2013) Dysbiosis of bifidobacteria and Clostridium cluster XIVa in the cystic fibrosis fecal microbiota. J Cyst Fibros 12:206–215

Edgar RC, Haas BJ, Clemente JC, Quince C, Knight R (2011) UCHIME improves sensitivity and speed of chimera detection. Bioinformatics 27:2194–2200

Evans J, Sheneman L, Foster J (2006) Relaxed neighbor joining: a fast distance-based phylogenetic tree construction method. J Mol Evol 62:785–792

Filkins LM, Hampton TH, Gifford AH, Gross MJ, Hogan DA, Sogin ML, Morrison HG, Paster BJ, O'Toole GA (2012) Prevalence of streptococci and increased polymicrobial diversity associated with cystic fibrosis patient stability. J Bacteriol 194:4709–4717

French PJ, van Doorninck JH, Peters RH, Verbeek E, Ameen NA, Marino CR, de Jonge HR, Bijman J, Scholte BJ (1996) A delta F508 mutation in mouse cystic fibrosis transmembrane conductance regulator results in a temperature-sensitive processing defect in vivo. J Clin Invest 98:1304–1312

Fridge JL, Conrad C, Gerson L, Castillo RO, Cox K (2007) Risk factors for small bowel bacterial overgrowth in cystic fibrosis. J Pediatr Gastroenterol Nutr 44:212–218

Gallagher AM, Gottlieb RA (2001) Proliferation, not apoptosis, alters epithelial cell migration in small intestine of CFTR null mice. Am J Physiol Gastrointest Liver Physiol 281:G681–G687

Gavina M, Luciani A, Villella VR, Esposito S, Ferrari E, Bressani I, Casale A, Bruscia EM, Maiuri L, Raia V (2013) Nebulized hyaluronan ameliorates lung inflammation in cystic fibrosis mice. Pediatr Pulmonol 48:761–771

Goddard AF, Staudinger BJ, Dowd SE, Joshi-Datar A, Wolcott RD, Aitken ML, Fligner CL, Singh PK (2012) Direct sampling of cystic fibrosis lungs indicates that DNA-based analyses of upper-airway specimens can misrepresent lung microbiota. Proc Natl Acad Sci USA 109:13769–13774

Haston CK, Corey M, Tsui LC (2002) Mapping of genetic factors influencing the weight of cystic fibrosis knockout mice. Mamm Genome 13:614–618

Haston CK, Cory S, Lafontaine L, Dorion G, Hallett MT (2006) Strain-dependent pulmonary gene expression profiles of a cystic fibrosis mouse model. Physiol Genomics 25:336–345

Hildebrand F, Nguyen TL, Brinkman B, Yunta RG, Cauwe B, Vandenabeele P, Liston A, Raes J (2013) Inflammation-associated enterotypes, host genotype, cage and inter-individual effects drive gut microbiota variation in common laboratory mice. Genome Biol 14:R4

Hoffman LR, Pope CE, Hayden HS, Heltshe S, Levy R, McNamara S, Jacobs MA, Rohmer L, Radey M, Ramsey BW, Brittnacher MJ, Borenstein E, Miller SI (2014) *Escherichia coli* dysbiosis correlates with gastrointestinal dysfunction in children with cystic fibrosis. Clin Infect Dis 58:396–399

Human Microbiome Project C (2012) Structure, function and diversity of the healthy human microbiome. Nature 486:207–214

Ivanov II, Atarashi K, Manel N, Brodie EL, Shima T, Karaoz U, Wei D, Goldfarb KC, Santee CA, Lynch SV, Tanoue T, Imaoka A, Itoh K, Takeda K, Umesaki Y, Honda K, Littman DR (2009) Induction of intestinal Th17 cells by segmented filamentous bacteria. Cell 139:485–498

Kent G, Oliver M, Foskett JK, Frndova H, Durie P, Forstner J, Forstner GG, Riordan JR, Percy D, Buchwald M (1996) Phenotypic abnormalities in long-term surviving cystic fibrosis mice. Pediatr Res 40:233–241

Kreda SM, Davis CW, Rose MC (2012) CFTR, mucins, and mucus obstruction in cystic fibrosis. Cold Spring Harb Perspect Med 2:a009589

Lappinga PJ, Abraham SC, Murray JA, Vetter EA, Patel R, Wu TT (2010) Small intestinal bacterial overgrowth: histopathologic features and clinical correlates in an underrecognized entity. Arch Pathol Lab Med 134:264–270

Lisowska A, Wojtowicz J, Walkowiak J (2009) Small intestine bacterial overgrowth is frequent in cystic fibrosis: combined hydrogen and methane measurements are required for its detection. Acta Biochim Pol 56:631–634

Liu J, Walker NM, Cook MT, Ootani A, Clarke LL (2012) Functional Cftr in crypt epithelium of organotypic enteroid cultures from murine small intestine. Am J Physiol Cell Physiol 302:C1492–C1503

Lubamba B, Lebacq J, Lebecque P, Vanbever R, Leonard A, Wallemacq P, Leal T (2009) Airway delivery of low-dose miglustat normalizes nasal potential difference in F508del cystic fibrosis mice. Am J Respir Crit Care Med 179:1022–1028

Lynch SV, Goldfarb KC, Wild YK, Kong W, De Lisle RC, Brodie EL (2013) Cystic fibrosis transmembrane conductance regulator knockout mice exhibit aberrant gastrointestinal microbiota. Gut Microbes 4:41–47

Madan JC, Koestler DC, Stanton BA, Davidson L, Moulton LA, Housman ML, Moore JH, Guill MF, Morrison HG, Sogin ML, Hampton TH, Karagas MR, Palumbo PE, Foster JA, Hibberd PL, O'Toole GA (2012) Serial analysis of the gut and respiratory microbiome in cystic fibrosis in infancy: interaction between intestinal and respiratory tracts and impact of nutritional exposures. MBio 3(4):e00251–12

Malmberg EK, Noaksson KA, Phillipson M, Johansson ME, Hinojosa-Kurtzberg M, Holm L, Gendler SJ, Hansson GC (2006) Increased levels of mucins in the cystic fibrosis mouse small intestine, and modulator effects of the Muc1 mucin expression. Am J Physiol Gastrointest Liver Physiol 291:G203–G210

Norkina O, Burnett TG, De Lisle RC (2004) Bacterial overgrowth in the cystic fibrosis transmembrane conductance regulator null mouse small intestine. Infect Immun 72:6040–6049

O'Connor A, Quizon PM, Albright JE, Lin FT, Bennett BJ (2014) Responsiveness of cardiometabolic-related microbiota to diet is influenced by host genetics. Mamm Genome 25:583–599

O'Sullivan BP, Freedman SD (2009) Cystic fibrosis. Lancet 373:1891–1904

Ott SJ, Musfeldt M, Ullmann U, Hampe J, Schreiber S (2004) Quantification of intestinal bacterial populations by real-time PCR with a universal primer set and minor groove binder probes: a global approach to the enteric flora. J Clin Microbiol 42:2566–2572

Paradis J, Wilke M, Haston CK (2010) Osteopenia in Cftr-deltaF508 mice. J Cyst Fibros 9:239–245

Preidis GA, Saulnier DM, Blutt SE, Mistretta TA, Riehle KP, Major AM, Venable SF, Finegold MJ, Petrosino JF, Conner ME, Versalovic J (2012) Probiotics stimulate enterocyte migration and microbial diversity in the neonatal mouse intestine. FASEB J 26:1960–1969

Pruesse E, Quast C, Knittel K, Fuchs BM, Ludwig W, Peplies J, Glockner FO (2007) SILVA: a comprehensive online resource for quality checked and aligned ribosomal RNA sequence data compatible with ARB. Nucleic Acids Res 35:7188–7196

Putney LK, Barber DL (2003) Na-H exchange-dependent increase in intracellular pH times G2/M entry and transition. J Biol Chem 278:44645–44649

Quince C, Lanzen A, Curtis TP, Davenport RJ, Hall N, Head IM, Read LF, Sloan WT (2009) Accurate determination of microbial diversity from 454 pyrosequencing data. Nat Methods 6:639–641

Rehman A, Sina C, Gavrilova O, Hasler R, Ott S, Baines JF, Schreiber S, Rosenstiel P (2011) Nod2 is essential for temporal development of intestinal microbial communities. Gut 60: 1354–1362

Risse PA, Kachmar L, Matusovsky OS, Novali M, Gil FR, Javeshghani S, Keary R, Haston CK, Michoud MC, Martin JG, Lauzon AM (2012) Ileal smooth muscle dysfunction and remodeling in cystic fibrosis. Am J Physiol Gastrointest Liver Physiol 303:G1–G8

Russell SL, Gold MJ, Hartmann M, Willing BP, Thorson L, Wlodarska M, Gill N, Blanchet MR, Mohn WW, McNagny KM, Finlay BB (2012) Early life antibiotic-driven changes in microbiota enhance susceptibility to allergic asthma. EMBO Rep 13:440–447

Scanlan PD, Buckling A, Kong W, Wild Y, Lynch SV, Harrison F (2012) Gut dysbiosis in cystic fibrosis. J Cyst Fibros 11:454–455

Schloss PD, Westcott SL, Ryabin T, Hall JR, Hartmann M, Hollister EB, Lesniewski RA, Oakley BB, Parks DH, Robinson CJ, Sahl JW, Stres B, Thallinger GG, Van Horn DJ, Weber CF (2009) Introducing mothur: open-source, platform-independent, community-supported software for describing and comparing microbial communities. Appl Environ Microbiol 75:7537–7541

Schloss PD, Gevers D, Westcott SL (2011) Reducing the effects of PCR amplification and sequencing artifacts on 16S rRNA-based studies. PLoS ONE 6:e27310

Snouwaert JN, Brigman KK, Latour AM, Malouf NN, Boucher RC, Smithies O, Koller BH (1992) An animal model for cystic fibrosis made by gene targeting. Science 257:1083–1088

Sun X, Olivier AK, Liang B, Yi Y, Sui H, Evans TI, Zhang Y, Zhou W, Tyler SR, Fisher JT, Keiser NW, Liu X, Yan Z, Song Y, Goeken JA, Kinyon JM, Fligg D, Wang X, Xie W, Lynch TJ, Kaminsky PM, Stewart ZA, Pope RM, Frana T, Meyerholz DK, Parekh K, Engelhardt JF (2014a) Lung phenotype of juvenile and adult cystic fibrosis transmembrane conductance regulator-knockout ferrets. Am J Respir Cell Mol Biol 50:502–512

Sun X, Olivier AK, Yi Y, Pope CE, Hayden HS, Liang B, Sui H, Zhou W, Hager KR, Zhang Y, Liu X, Yan Z, Fisher JT, Keiser NW, Song Y, Tyler SR, Goeken JA, Kinyon JM, Radey MC, Fligg D, Wang X, Xie W, Lynch TJ, Kaminsky PM, Brittnacher MJ, Miller SI, Parekh K, Meyerholz DK, Hoffman LR, Frana T, Stewart ZA, Engelhardt JF (2014b) Gastrointestinal pathology in juvenile and adult CFTR-knockout ferrets. Am J Pathol 184:1309–1322

van der Doef HP, Kokke FT, van der Ent CK, Houwen RH (2011) Intestinal obstruction syndromes in cystic fibrosis: meconium ileus, distal intestinal obstruction syndrome, and constipation. Curr Gastroenterol Rep 13:265–270

van der Wulp MY, Derrien M, Stellaard F, Wolters H, Kleerebezem M, Dekker J, Rings EH, Groen AK, Verkade HJ (2013) Laxative treatment with polyethylene glycol decreases microbial primary bile salt dehydroxylation and lipid metabolism in the intestine of rats. Am J Physiol Gastrointest Liver Physiol 305:G474–G482

van Doorninck JH, French PJ, Verbeek E, Peters RH, Morreau H, Bijman J, Scholte BJ (1995) A mouse model for the cystic fibrosis delta F508 mutation. EMBO J 14:4403–4411

Wang Q, Garrity GM, Tiedje JM, Cole JR (2007) Naive Bayesian classifier for rapid assignment of rRNA sequences into the new bacterial taxonomy. Appl Environ Microbiol 73:5261–5267

White JR, Nagarajan N, Pop M (2009) Statistical methods for detecting differentially abundant features in clinical metagenomic samples. PLoS Comput Biol 5:e1000352

Wilke M, Buijs-Offerman RM, Aarbiou J, Colledge WH, Sheppard DN, Touqui L, Bot A, Jorna H, de Jonge HR, Scholte BJ (2011) Mouse models of cystic fibrosis: phenotypic analysis and research applications. J Cyst Fibros 10:S152–S171

Yu Z, Morrison M (2004) Improved extraction of PCR-quality community DNA from digesta and fecal samples. Biotechniques 36:808–812

Zhao J, Liao D, Yang J, Gregersen H (2010) Biomechanical remodelling of obstructed guinea pig jejunum. J Biomech 43:1322–1329

Zhao J, Schloss PD, Kalikin LM, Carmody LA, Foster BK, Petrosino JF, Cavalcoli JD, VanDevanter DR, Murray S, Li JZ, Young VB, LiPuma JJ (2012) Decade-long bacterial community dynamics in cystic fibrosis airways. Proc Natl Acad Sci U S A 109:5809–5814